NASA/TM—2020-220499

Microwave Photoelasticity: A Resonant Wavelength Approach Applied to PEEK Polymer

Peter J. Schemmel and Seth W. Waldstein
Glenn Research Center, Cleveland, Ohio

March 2020

NASA STI Program . . . in Profile

Since its founding, NASA has been dedicated to the advancement of aeronautics and space science. The NASA Scientific and Technical Information (STI) Program plays a key part in helping NASA maintain this important role.

The NASA STI Program operates under the auspices of the Agency Chief Information Officer. It collects, organizes, provides for archiving, and disseminates NASA's STI. The NASA STI Program provides access to the NASA Technical Report Server—Registered (NTRS Reg) and NASA Technical Report Server—Public (NTRS) thus providing one of the largest collections of aeronautical and space science STI in the world. Results are published in both non-NASA channels and by NASA in the NASA STI Report Series, which includes the following report types:

- TECHNICAL PUBLICATION. Reports of completed research or a major significant phase of research that present the results of NASA programs and include extensive data or theoretical analysis. Includes compilations of significant scientific and technical data and information deemed to be of continuing reference value. NASA counter-part of peer-reviewed formal professional papers, but has less stringent limitations on manuscript length and extent of graphic presentations.

- TECHNICAL MEMORANDUM. Scientific and technical findings that are preliminary or of specialized interest, e.g., "quick-release" reports, working papers, and bibliographies that contain minimal annotation. Does not contain extensive analysis.

- CONTRACTOR REPORT. Scientific and technical findings by NASA-sponsored contractors and grantees.

- CONFERENCE PUBLICATION. Collected papers from scientific and technical conferences, symposia, seminars, or other meetings sponsored or co-sponsored by NASA.

- SPECIAL PUBLICATION. Scientific, technical, or historical information from NASA programs, projects, and missions, often concerned with subjects having substantial public interest.

- TECHNICAL TRANSLATION. English-language translations of foreign scientific and technical material pertinent to NASA's mission.

For more information about the NASA STI program, see the following:

- Access the NASA STI program home page at http://www.sti.nasa.gov

- E-mail your question to help@sti.nasa.gov

- Fax your question to the NASA STI Information Desk at 757-864-6500

- Telephone the NASA STI Information Desk at 757-864-9658

- Write to:
  NASA STI Program
  Mail Stop 148
  NASA Langley Research Center
  Hampton, VA 23681-2199

NASA/TM—2020-220499

Microwave Photoelasticity: A Resonant Wavelength Approach Applied to PEEK Polymer

Peter J. Schemmel and Seth W. Waldstein
Glenn Research Center, Cleveland, Ohio

National Aeronautics and
Space Administration

Glenn Research Center
Cleveland, Ohio 44135

March 2020

Acknowledgments

This work is supported by the NASA, Aeronautics Research Mission Directorate, Transformational Tools and Technologies Project.

This work was sponsored by the
Transformative Aeronautics Concepts Program.

Level of Review: This material has been technically reviewed by technical management.

Available from

NASA STI Program
Mail Stop 148
NASA Langley Research Center
Hampton, VA 23681-2199

National Technical Information Service
5285 Port Royal Road
Springfield, VA 22161
703-605-6000

This report is available in electronic form at http://www.sti.nasa.gov/ and http://ntrs.nasa.gov/

Microwave Photoelasticity: A Resonant Wavelength Approach Applied to PEEK Polymer

Peter J. Schemmel and Seth W. Waldstein
National Aeronautics and Space Administration
Glenn Research Center
Cleveland, Ohio 44135

Abstract

Every nondestructive testing (NDT) technique has its unique set of advantages and limitations. Currently, the only existing noncontact NDT method capable of measuring sub-surface stresses, in optically opaque materials, at near-real-time speeds and over large areas is Microwave Photoelasticity (MP). This paper presents a new MP approach, which correlates changes in resonant wavelengths to changes in stress. In addition to a theoretical outline of the approach, the design and operation of an instrument capable of conducting these measurements is described. Finally, the technique is demonstrated by conducting measurements on polyetheretherketone, commonly known as PEEK, polymer. Between the W-Band frequencies of 105 to 115 GHz, PEEK's stress-optic-coefficient was determined to be of $C = -0.20 \pm 0.02$ 1/GPa.

1.0 Introduction and Motivation

Today, engineers have access to numerous testing methods capable of measuring stresses within materials. Each method possesses a particular set characteristics making it well-suited to specific applications. Traditional strain gauges excel at high-precision, single point measurements, while digital image correlation (DIC) is superior when analyzing dynamic stress distributions. Residual stress analysis often utilizes a variety of X-Ray diffraction (XRD) techniques. Yet, each technique also has a set of limitations.

These limitations ultimately restrict the ability to assess material performance under certain conditions. For example, high-temperature testing degrades surface treatments required by traditional strain gauges and DIC applications. Ionizing X-Rays are potentially harmful to the integrity of the test materials, and XRD is further limited to the analysis of small spatial regions. Alternative destructive testing techniques are not cost-effective and ill-suited to quality control applications where individual components are intended to be entered into service (Ref. 1). Therefore, it is necessary to continue developing new nondestructive testing (NDT) methods that complement existing techniques.

This paper describes a NDT technique capable of measuring stresses by utilizing focused beams of microwave radiation (Refs. 2 to 4). The technique, similar to radar, operates by identifying and tracking wavelength (or frequency) resonances generated by the interaction of the microwave beam and material under test. Focused microwave radiation is capable of imaging full-field stress distributions as well as measuring sub-surface stresses. Additionally, since the technique does not require any contact with, or modification of the material, it is well-suited to both high-temperature testing and quality control applications.

Section 2.0 of this paper describes the theoretical foundation on which the resonant wavelength technique is built, while Section 3.0 describes an instrument capable of conducting these measurements. Finally, Section 4.0 demonstrates how the technique works in practice by providing measurement data obtained from polyetheretherketone (PEEK) polymer (Ref. 5).

2.0 Using Resonant Wavelengths to Measure Stress

Materials under stress become birefringent, meaning that their refractive index changes in both direction and magnitude. The stress-optic-law (Ref. 6) states that the level of birefringence is linearly proportional to the difference in stress along the material's principle stress axis. The stress-optic-law is commonly written as (Ref. 2),

$$\Delta n = C\Delta\sigma \tag{1}$$

Here, Δn is the change in refractive index, C is the stress-optic-coefficient (SOC) and $\Delta\sigma$ is the change in stress applied to the material. The use of visible light to measure stress distributions in materials, via Equation (1), is known as photoelasticity.

Photoelastic measurements were vital to aerospace engineering before the advent of computer-aided-design or CAD (Ref. 7). The technique allowed engineers to quickly visualize component performance under load, and enabled rapid optimization of designs. However, traditional photoelastic measurements require visible light, limiting the technique to optically transparent materials, few of which are relevant to aerospace applications (Ref. 8).

Today, microwave technologies are in widespread use. Vector network analyzers (VNAs) now regularly support frequencies from 100 GHz up to several THz. Importantly, microwaves are transparent to a number of high-value materials used in aerospace applications, and are still able to produce images with high spatial resolution. These characteristics make today's high-frequency microwave instruments capable of imaging refractive index distribution across aerospace engineering materials.

One method to measure the refractive index of a material is to measure its resonant wavelength (or frequency) (Ref. 9). This approach relies on the Fabry-Perot effect, where propagating electromagnetic waves are partially transmitted and reflected at the boundaries between two materials. In the case of a dielectric slab with parallel faces, constructive and destructive interference takes place between the partially transmitted and reflected waves from the slab's front and back surfaces (Ref. 10).

Both the Fabry-Perot transmission and reflection coefficients are analytically determined by a nonlinear equation (Refs. 2 and 3). Analysis of the nonlinear equations shows that the points of maximum transmission (and hence minimum reflection) are described by (Ref. 9),

$$n \cdot d = \frac{\alpha}{2}\lambda_0 \tag{2}$$

where d is the dielectric slab's thickness, λ_o is the wavelength corresponding to the minimum reflected power (i.e., the resonant wavelength), and α is an integer that is equal to the number of half-wavelengths within the material.

Therefore, a change in refractive index must result in resonant wavelength change such that,

$$\Delta\lambda_0 = \frac{2d}{\alpha} \cdot \Delta n \tag{3}$$

Substitution of Equation (1) into Equation (3) then yields,

$$\Delta\lambda_0 = \frac{2d}{\alpha} \cdot C\Delta\sigma \tag{4}$$

For standard dogbone shaped specimens, the change in stress is simply the ratio of the change in applied load to cross sectional area.

$$\Delta\lambda_0 = \frac{2C}{\alpha \cdot w} \cdot \Delta F \tag{5}$$

Here, ΔF is the change in applied load, and w is the specimen width. Note that the specimen thickness d drops out of the equation. Note that C has units of m^2/N, or $1/Pa$, (better known as a Brewster) which is the same as was used in traditional visible photoelastic systems. After examining Equation (5) it is clear that when measuring dogbone shaped specimens, the resonant wavelength will change as a linear function of the applied load. A measurement system used to determine the relationship between resonant wavelength and applied force, is described in the upcoming Section.

3.0 Measurement System Overview

The resonant wavelength approach outlined in Section 2.0 requires the generation and receipt of a free-space microwave beam that is normally incident to the material under test. Furthermore, identification of the resonant wavelength necessitates a frequency-domain approach. A suitable solution is to utilize a quasi-optical set up, whereby mirrors or lenses focus radiation from an antenna onto the sample (Ref. 11).

Figure 1 shows the quasi-optical set up used to gather all experimental data used in this paper. The instrument consists of two antennas, with polytetrafluoroethylene (PTFE) lenses that focus the microwave beam onto the specimen. A tensile testing stage is used to apply tensile loads to dogbone shaped specimens. Each antenna is connected to a VNA which supplies the transmission signal and records the received signal across a designated frequency band. By comparing the transmitted and received signals, the VNA calculates four scattering, or S-parameters. These S-parameters indicate the signal received by antenna 1 due to the signal from antenna 1 (S_{11}), the signal received by antenna 2 due to the signal from antenna 1 (S_{21}), and so forth (Ref. 12).

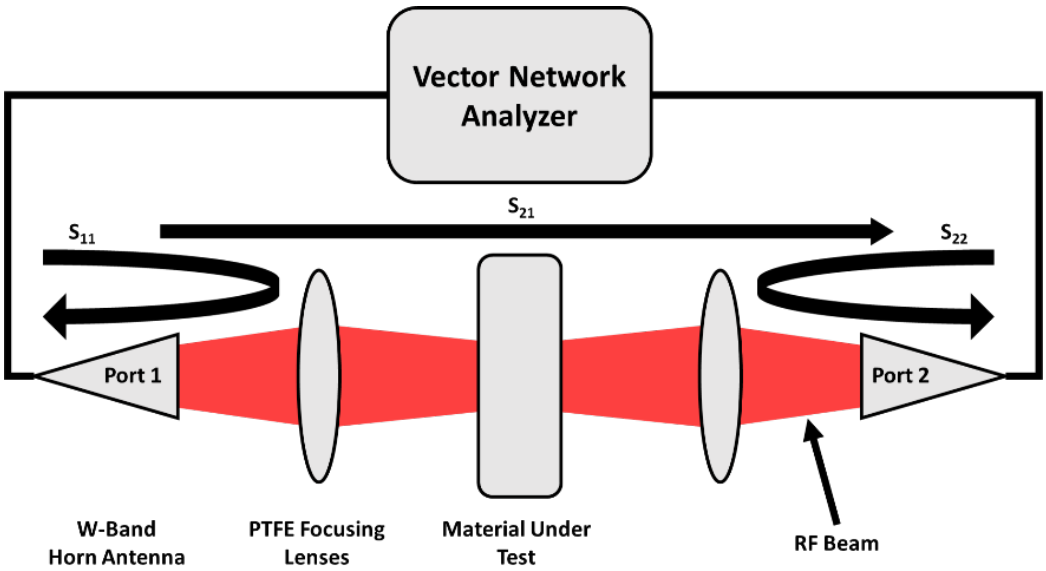

Figure 1.—Diagram of the microwave instrument used to collect data in this paper. A VNA produces a microwave signal which is focused onto the material under test, using PTFE lenses. The VNA captures the resulting S-Parameters, which are used to identify and track resonances.

Acquiring accurate S-parameter data necessitates that the VNA be calibrated. While there are numerous VNA calibration procedures, a commonly used method for free-space applications is known as Thru-Reflect-Match (TRM) (Refs. 13 and 14). This procedure consists of three separate measurements, the first of which is the Thru-measurement. Thru measurements are completed by recording the four S-parameters without a specimen present. Reflect measurements are completed by placing a polished flat mirror, with the same dimensions as the eventual test specimens, in the sample holder, and again recording all four S-parameters. Finally, the Match measurement consists of measuring the S-parameters produced when microwave absorber is placed in the specimen location. Modern VNAs typically contain software to automatically calculate the calibration coefficients, alternatively they may be determined manually (Ref. 11). Finally, a time-gate is applied to the calibrated data, so that spurious reflections from objects other than the material under test are removed from the S-parameter data.

Calibrated S-parameter data (Figure 2), as well as the current applied load and specimen extension, is collected from the VNA and tensile stage using a remote computer. An analysis program is used to calculate the resonant wavelength from the reflection (S_{11} or S_{22}) data. The first step is to determine the frequency associated with the minimum reflection magnitude. Then, a quadratic fit is applied to the data points nearest the initial resonant frequency value. A revised minimum S-parameter magnitude is identified (Figure 3). Important VNA parameters used to collect data presented in this paper are displayed in Table 1.

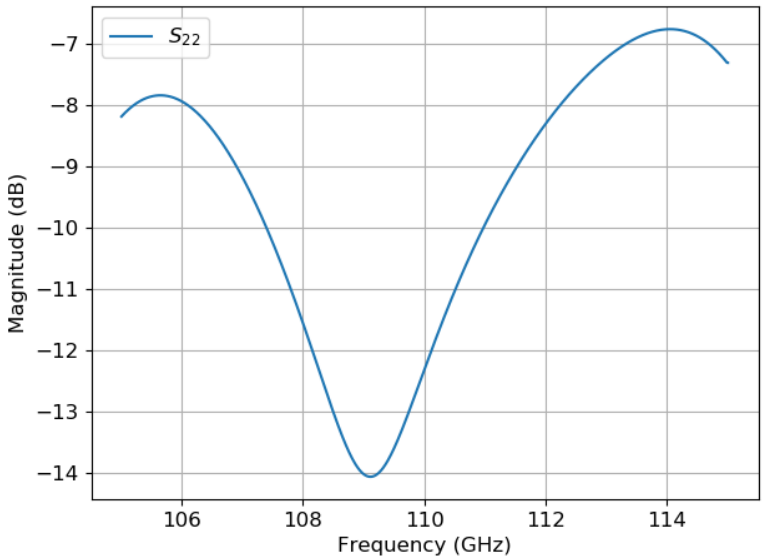

Figure 2.—S-parameter data, collected by the VNA, includes resonances in the reflection coefficient.

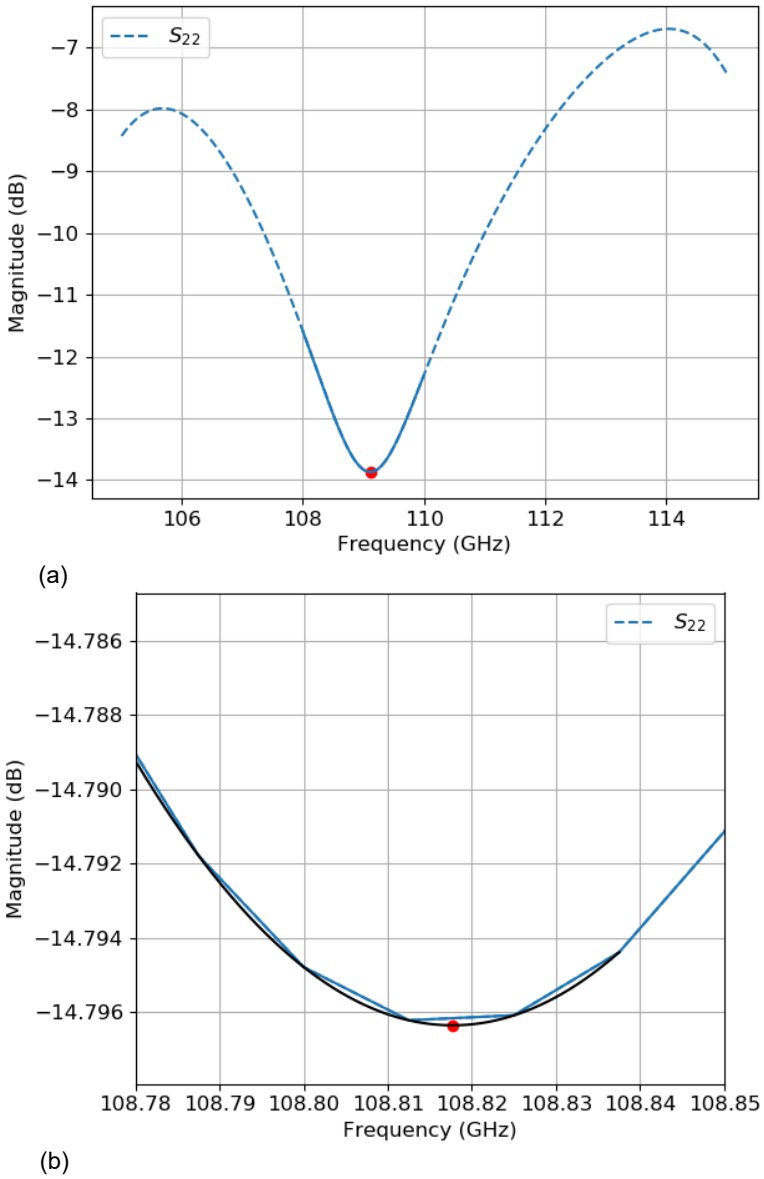

Figure 3.—Resonances are identified by locating minima in the measured reflection coefficient. Initially, the minimum magnitude in the measured array is identified using an analysis script (a). This course identification is refined by fitting a quadratic function to the measured data, in the region of the initial resonance value (b). (a) Course identification of the resonant frequency. (b) Refinement of the resonant frequency identification.

TABLE 1.—VNA PARAMETERS USED TO COLLECT DATA PRESENTED IN THIS PAPER

Parameter name	Value	Units
Frequency start	105	GHz
Frequency stop	115	GHz
Number of frequency points	801	---
Frequency spacing	12.5	MHz
Intermediate frequency bandwidth	300	Hz
Time gate start	–100	ps
Time gate stop	+100	ps

4.0 PEEK Polymer Results

Polyaryletherketone, or PEEK, is a thermoplastic polymer commonly used in aerospace applications. PEEK is well behaved from both a mechanical and RF perspective. For example, PEEK has a tensile modulus of 3.7 GPa and a tensile strength of 100 MPa (Ref. 5). From an RF perspective, PEEK has a negligible loss tangent and a modest refractive index of $n = 1.79$ (Ref. 15). Sub-Section 4.1 describes the process for determining α, used in Equation (5). PEEK's stress-optic-coefficient is determined in Section 4.2 while the impact of varying specimen width is shown in Section 4.3.

4.1 Determining α

Section 2.0 described a technique to measure stresses within dielectric materials by identifying and tracking resonant wavelengths generated by destructive interference induced by the material under test. This technique depends, in part, on the identification of the number of half-wavelengths α, within the material.

Determining the appropriate value for α begins by measuring the reflection coefficient of the material (S_{11} or S_{22}), and identifying the resonant wavelength. Figure 3 indicates that a 3.08 mm thick slab of PEEK material produces a resonant frequency at 109.114 GHz, which translates to a resonant wavelength of $\lambda_0 = 2.75$ mm. Rearranging Equation (2) yields the useful equation,

$$\alpha = int\left(\frac{2n \cdot d}{\lambda_0}\right) \tag{6}$$

Here, $int(\,)$ specifies that noninteger quotients shall be rounded to the nearest integer. A value of $\alpha = 4$ is achieved by using PEEKs known refractive index, across W-Band (75 to 110 GHz) of $n = 1.79$ (Ref. 15).

The value of α is confirmed by using the following rearrangement of Equation (2), which results in a redetermined thickness of 3.07 mm.

$$d = \frac{\alpha \cdot \lambda_0}{2n} \tag{7}$$

This 10 μm difference from the actual measured sample thickness is well within the expected error associated with using a digital hand caliper. Now that α is known, PEEK's stress-optic-coefficient C, may be determined.

4.2 Determining the Stress Optic Coefficient

Several steps are required to measure a material's stress-optic-coefficient. First, tensile testing specimens must be subjected to several applied loads. Here, PEEK specimens were placed under an incrementally increasing tensile load, up to a maximum of 1,200 N, and then subsequently relaxed incrementally back to a load-free condition. This process was repeated three times as demonstrated by Figure 4(a). An extensometer was used in conjunction with the tensile testing machine's load cell, producing force versus head displacement curves (Figure 4(b)) across the entire load-profile.

As the tensile testing stage steps through each load point, the VNA (Figure 1) captures S-Parameters generated by the interaction of the microwave beam and material. The next step in the process is to determine the resonant wavelength from either S_{11} or S_{22}, using the process outlined in Section 4.1, and then plot that resonant wavelength as a function of the applied force. Figure 5(a) shows the accumulated results of this process, generated by five PEEK specimens. A linear fit (dashed line) is then applied to each set of data points resulting in a measured slope and y-intercept for each individual specimen.

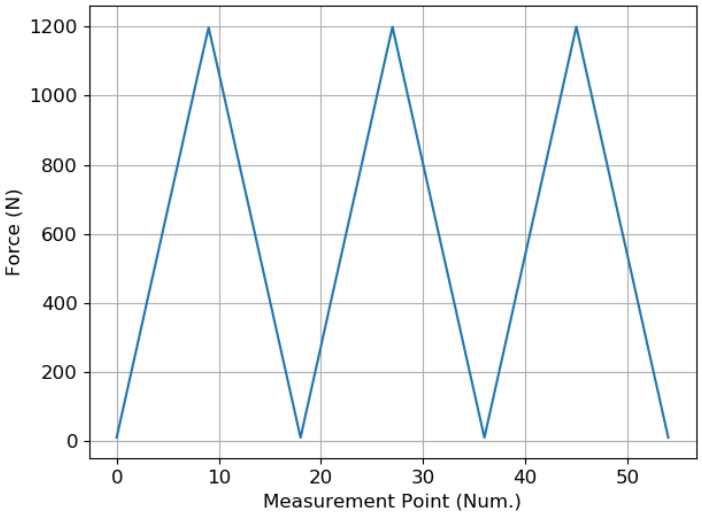

(a)

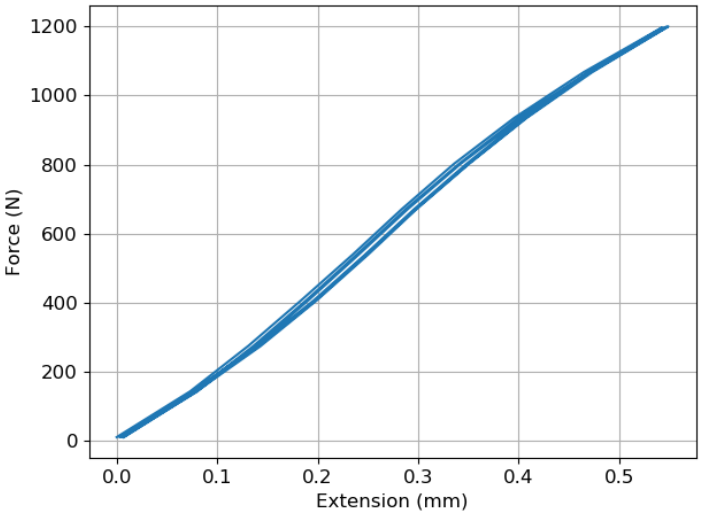

(b)

Figure 4.—PEEK specimens were subjected to a linear loading ramp, up to a maximum of 1,200 N, three times (a). Specimens exhibited elastic behavior during the test, as observed by the repeatable force versus head displacement traces (b). (a) Loading cycle as a function of time. (b) Force versus head displacement.

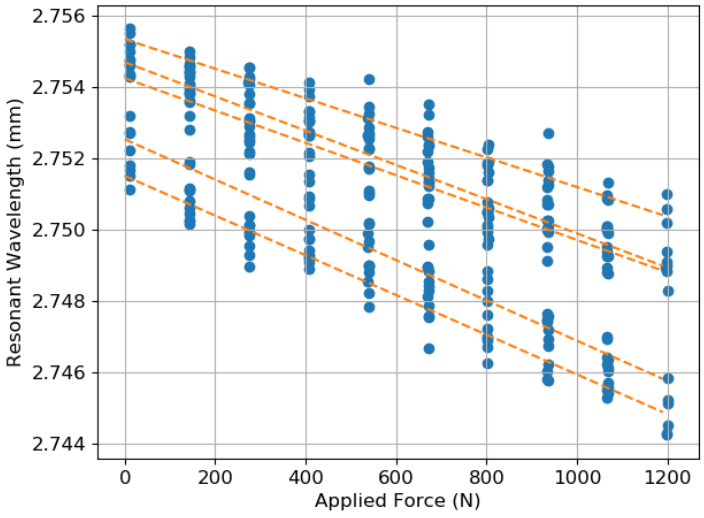

(a)

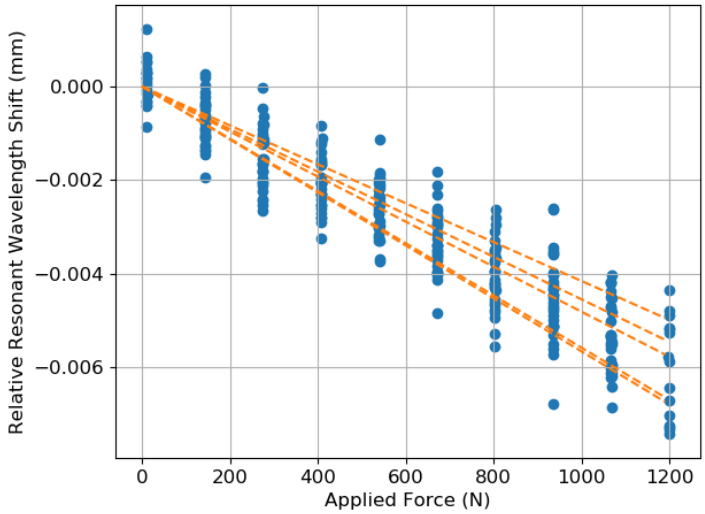

(b)

Figure 5.—Resonant wavelength is a linear function of applied force, as expected according to the Stress-Optic-Law (a). Small changes in the resonant wavelength, due to differences in VNA calibration, specimen placement and material properties, produce a vertical offset between data sets, which are removed to observe the relative change in resonant wavelength (b). (a) Absolute change in resonant wavelength versus applied force. (b) Relative change in resonant wavelength versus applied force.

The final step in determining the stress-optic-coefficient is to solve Equation (5). Since Equation (5) requires the change in resonant wavelength, the vertical shift between individual specimens is removed from Figure 5(a), resulting in Figure 5(b). Finally, note the PEEK specimens used in this study had gauge widths of 20 mm and recall that Section 4.1 determined that $\alpha = 4$. Therefore, Equation (5) may be rearranged to solve directly for the stress-optic-coefficient. Doing so results in a value of $C = -0.20 \pm 0.02$ 1/GPa.

4.3 Impact of Sample Width

It is evident from examining Equation (5), that measured resonant wavelengths depend on α, as described in Section 4.1, but also the sample width. In fact, the slope observed when plotting measured resonant wavelength versus applied force is inversely proportional to sample width. Therefore, when specimens of different widths are measured, their resonant wavelength versus applied force slopes $\left(\frac{2C}{\alpha \cdot w}\right)$ will be different. The critical point to remember is that it is the stress-optic-coefficient C, which is consistent for a material, not the measured slope of resonant wavelength versus applied force.

To demonstrate this fact, three PEEK specimens, each with different widths (15, 20, and 25 mm), were manufactured and subjected to the same load profile conducted in Section 4.2, four times each. The average response, complied from all four runs of each individual specimen are presented in Figure 6(a). It is clear that the three responses are different, and that the absolute value of the slope increases as the width decreases, which is expected according to Equation (5).

Figure 6(b), on the other hand, plots the following equation.

$$\frac{\Delta\lambda_0 \cdot w \cdot \alpha}{2} = C \cdot \Delta F \tag{8}$$

It is clear from the form of Equation (8) that the resulting slopes in Figure 6(b) should all be equivalent, as the constant of proportionality is just the stress-optic-coefficient, which is a material property. Inspection of Figure 6(b) confirms that this is indeed the case. Table 2 provides the values of each determined slope in Figure 6.

The values in the center column of Table 2 correspond to the slopes in Figure 6(a). The result is a different slope for specimens of different widths. Assuming a normal distribution, none of these results overlap sufficiently enough to claim that they are statistically similar. On the other hand, the right most column of Table 2 provides the determined stress-optic-coefficient for each specimen type, which are certainly from the same distribution.

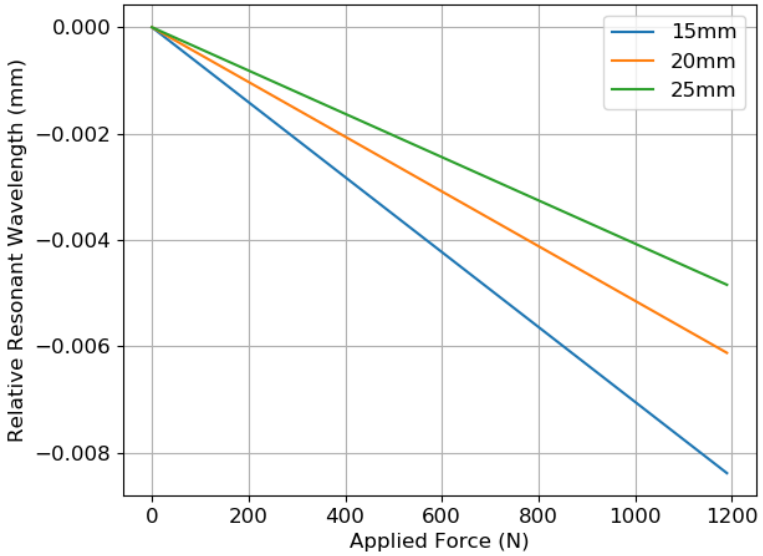

(a)

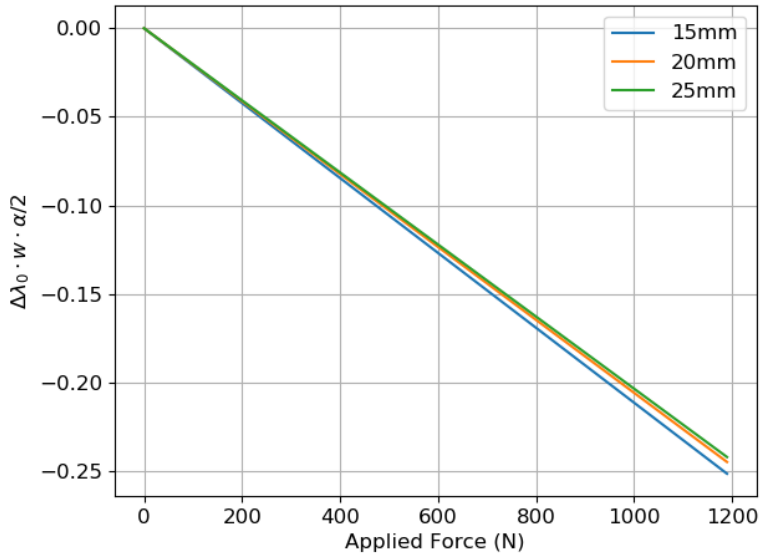

(b)

Figure 6.—As measured resonant wavelength is a function of both α and specimen width. Thus, the slopes produces when measuring specimens of different widths, will be different (a). Correcting the resonant wavelength, (Eq. (8)), results in a linear function with a slope equal to the stress-optic-coefficient C, for all specimen widths (b). (a) Measured resonant wavelengths not accounting for changes in width. (b) Corrected resonant wavelength versus applied force data.

TABLE 2.—MEASURED SLOPES FROM FIGURE 6, DEMONSTRATING THE IMPACT OF NOT CORRECTING FOR DIFFERENCES IN SPECIMEN WIDTHS, THUS VALIDATING EQUATION (5)

Sample width, mm	$\frac{2C}{\alpha \cdot w}$ (mm/N)	C (1/GPa)
15	–0.007 ± 0.0007	–0.21 ± 0.02
20	–0.005 ± 0.0005	–0.21 ± 0.02
25	–0.004 ± 0.0006	–0.20 ± 0.03

5.0 Conclusion

This paper outlined a new method to measure material stresses using focused microwave radiation and a resonant wavelength analysis approach. In Section 2.0, a new equation (Eq. (5)), connecting the Stress Optic Law and Fabry-Perot equation for minimum reflection, was derived. The equation enables conversions between microwave collected refractive index data and mechanical stress. The constant of proportionality is a function of the stress-optic-coefficient C, the number of half-microwave wavelengths α present in the sample and the sample width.

Section 3.0 provided a short description of the measurement system and recorded data. A microwave beam, generated by an antenna, is focused onto the material under test using a lens. A vector network analyzer (VNA) collects S-Parameters, which determine the amount of power transmitted through, and reflected by, the material. Since the specimens being tested are dogbone shaped with flat and parallel front and back surfaces, the reflected power contains resonances governed by the Fabry-Perot effect.

Section 4.0 demonstrated this new microwave measurement approach using PEEK polymer as a test material. Section 4.1 demonstrated a technique for using these resonances to determine the half-wavelength term α. The half-wavelength term depends on the material's physical thickness and known refractive index. Once α is known, the stress-optic-coefficient is determinable.

Five dogbone specimens were machined from PEEK sheet, and were then subjected to a series of increasing and decreasing load profiles (Figure 4). At several points, the microwave system took S-Parameter measurements. These measurements were used to determine the resonant wavelength, which was then plotted as a function of the applied force in Figure 5. From this data, PEEK's stress-optic-coefficient was found to be $C = -0.20 \pm 0.02$ 1/GPa.

Finally, Section 4.3 showed how changing specimen width results in a different resonant wavelength versus applied force response (Figure 6(a)). However, the stress-optic-coefficient remained constant (Figure 6(b)). Table 2 provided statistical data showing that indeed, the resonant wavelength versus applied force responses were from statistically different distributions, while the calculated stress-optic-coefficients were statistically from the same distribution.

The methods, tools and results presented herein confirm that this new resonant wavelength approach, using focused microwave-radiation, is capable of accurately measuring stresses within aerospace relevant materials. This new NDT approach has the potential to make challenging tests, such as high-temperature sub-surface stress measurements, possible. The second paper in this series "Microwave Photoelasticity: Exploiting Multiple Resonances to Measure Stress Changes within Yttria-Partially-Stabilized-Zirconia," delves deeper into the technique using ceramic materials.

References

1. Schemmel, Peter J.: Reducing Aviation Fuel Costs with Non-Destructive Testing. NASA/TM—2019-220165, 2019. http://ntrs.nasa.gov
2. Schemmel, P.; Diederich, G.; and Moore, A.J.: Direct Stress Optic Coefficient for YTZP Ceramic and PTFE at GHz Frequencies. Opt. Express, vol. 24, no. 8, 2016, pp. 8110–8119.
3. Schemmel, P.; Diederich, G.; and Moore, A.J: Measurement of Direct Strain Optoc Coefficient of YSZ Thermal Barrier Coatings at GHz Frequencies. Opt. Express, vol. 25, no. 17, 2017, pp. 19968–19980.
4. Schemmel, Peter; and Moore, Andrew J.: Monitoring Stress Changes in Carbon Fiber Reinforced Polymer Composites with GHz Radiation. Appl. Opt., vol. 56, no. 22, 2017, pp. 6405–6409.

5. VICTREX PEEK Material Properties Guide. https://www.victrex.com/~/media/literature/en/material-properties-guide_us-4-20.pdf Accessed Feb. 13, 2020.
6. Ramesh, K: Digital Photoelasticity Advanced Techniques and Applications, Springer, 2000.
7. Cheng, Y.F.: An Investigation of Residual Stresses in Tempered Glass Plates of Aircraft Windshields, J. Aircraft, vol. 6, no. 2, 1969, pp. 156–159.
8. Raju, Basava B.: Nondestructive Measurement of Residual Stresses in Aircraft Transparencies, https://apps.dtic.mil/dtic/tr/fulltext/u2/a218680.pdf Accessed Feb. 13, 2020.
9. Maffei, B., et al.: Implementation of a quasi-optical free-space s-parameter measurement system, Proc. 35th ESA Antenna Conference, 2013.
10. Chen, L.F., et al.: Microwave Electronics: Measurement and Materials Characterization. John Wiley & Sons, Hoboken, NJ, 2004.
11. Schultz, John W.: Focused Beam Methods: Measuring Microwave Materials in Free Space. 2012.
12. Hiebel, M.: Fundamentals of Vector Network Analysis. Rohde & Schwarz, Columbia, MD, 2007.
13. Gagnon, N., et al.: Low-Cost Free-Space Measurement of Dielectric Constant at Ka-Band. IEE P.-Microw. Anten. P., vol. 151, no. 3, 2004, pp. 271–276.
14. Fralick, Dion T.: W-Band Free Space Permittivity Measurement Setup for Candidate Radome Materials. NASA CR-201720, 1997. http://ntrs.nasa.gov.
15. Schemmel, P.J. and Lambert K.M.: Refractive Index of Polyaryletherketone (PEEK) at X- and W-Band, NASA/TM—2019-220223, 2019. http://ntrs.nasa.gov